



## OPEN ACCESS

## EDITED BY

Hongliang Ming,  
Institute of Metal Research (CAS), China

## REVIEWED BY

Yueling Guo,  
Beijing Institute of Technology, China  
Chao Xiang,  
Institute of Metal Research (CAS), China

## \*CORRESPONDENCE

Qin Zhou,  
qinzhou@mail.tsinghua.edu.cn

## SPECIALTY SECTION

This article was submitted to  
Environmental Degradation of Materials,  
a section of the journal  
Frontiers in Materials

RECEIVED 30 September 2022

ACCEPTED 31 October 2022

PUBLISHED 17 November 2022

## CITATION

Shu M, Sun Y, Zhou Q, Xiao J, Ma Z and  
Liu X (2022), Overview on performance  
degradation behavior of 20Cr25NiNb  
steel for gas cooled reactor cladding  
during service.  
*Front. Mater.* 9:1058045.  
doi: 10.3389/fmats.2022.1058045

## COPYRIGHT

© 2022 Shu, Sun, Zhou, Xiao, Ma and  
Liu. This is an open-access article  
distributed under the terms of the  
[Creative Commons Attribution License  
\(CC BY\)](https://creativecommons.org/licenses/by/4.0/). The use, distribution or  
reproduction in other forums is  
permitted, provided the original  
author(s) and the copyright owner(s) are  
credited and that the original  
publication in this journal is cited, in  
accordance with accepted academic  
practice. No use, distribution or  
reproduction is permitted which does  
not comply with these terms.

# Overview on performance degradation behavior of 20Cr25NiNb steel for gas cooled reactor cladding during service

Ming Shu<sup>1,2</sup>, Yongduo Sun<sup>1</sup>, Qin Zhou<sup>2\*</sup>, Jun Xiao<sup>1</sup>,  
Zhaodandan Ma<sup>1</sup> and Xiao Liu<sup>1</sup>

<sup>1</sup>Nuclear Power Institute of China (NPIC), Chengdu, China, <sup>2</sup>Institute of Nuclear and New Energy Technology, Tsinghua University, Beijing, China

In this paper, the performance degradation behavior of fuel cladding material 20Cr25NiNb for the British Advanced Gas Reactor (AGR) is reviewed in detail, which is a strong guideline for the material selection of supercritical carbon dioxide cooled reactors. The degradation behavior during in-core service mainly includes high-temperature creep, thermal aging and mechanical property degradation caused by neutron irradiation (fission gas products, helium embrittlement and irradiation sensitization) and CO<sub>2</sub> (oxidation and carburizing). Long-term service in AGR leads to coarsening of the second phase and precipitation of harmful phases such as  $\sigma$ , leading to performance degradation of the cladding. A point that should require special attention is that intergranular stress corrosion cracking (IGSCC) and intergranular attack (IGA) problems occur during wet storage of spent fuel.

## KEYWORDS

20Cr25NiNb, AGR, cladding, austenitic heat resistant steel, performance degradation, irradiation, carbon dioxide

## 1 Introduction

Nuclear energy is an important part of global energy, characterized by low carbon emissions, safety and control, and high energy density (Wang et al., 2016). Systems using supercritical carbon dioxide (sCO<sub>2</sub>) as the heat transfer medium have the advantages of high energy conversion efficiency, simple system and small size (Dostál, 2004), which leads to extensive research carried out on the application of sCO<sub>2</sub> in nuclear reactors. Austenitic heat resistant steels at high temperatures have good mechanical properties, oxidation resistance and creep properties, which make them important candidates for sCO<sub>2</sub> reactors (Cao et al., 2012; Holcomb et al., 2016). It is obviously a better strategy to research and development cladding material of sCO<sub>2</sub> reactor based on the materials of AGR with service experience. The heat transfer medium of the AGR primary circuit adopts CO<sub>2</sub> with a pressure of 4 MPa (Dawson and Phillips, 2012) (sCO<sub>2</sub> reactor has a higher design pressure, up to 20 MPa), and the average temperature at the core outlet is up to 650°C (JIANG, 2018), with the transient peak temperature at the cladding position over 850°C (Evans, 1988). To summarize the performance degradation behavior of

TABLE 1 Range of main elements of 20Cr25NiNb for AGR cladding (Norris et al., 1992; Evans and Donaldson, 1998).

| Element | Content (wt%)          | Note  |
|---------|------------------------|---|
| Ni      | 24–26                  | The content of C, N and Nb in the later stage can also be referred to the following composition range (wt%): $10 \times C < Nb < 0.7$ ; C:0.01–0.05; N: no special provisions, usually 0.005–0.01 |
| Cr      | 19–21                  |   |
| Nb      | $\leq 0.8, > 8(C + N)$ |   |
| Si      | 0.45–0.75              |   |
| Mn      | 0.55–0.85              |   |
| C       | C + N:<br>0.040–0.080  |   |
| N       |                        |   |
| Ti      | <0.05                  |   |
| B       | <0.001                 |   |
| Co      | <0.015                 |   |
| S       | <0.02                  |   |
| P       | <0.02                  |   |
| Fe      | Bal                    |   |

cladding material 20Cr25NiNb for AGR is of great significance for sCO<sub>2</sub> gas-cooled reactor's design and cladding material selection.

## 2 AGR fuel cladding

### 2.1 Composition

The AGR core consists of approximately 81,600 fuel pins (Haynes et al., 2018) that are of a ribbed design (Whillock et al., 2018) and filled with helium to avoid additional fuel oxidation (Dawson and Phillips, 2012). On the basis of 310 stainless steel with adding a small amount of niobium “trapping” free C element in the matrix to avoid the intergranular corrosion, 20Cr25NiNb stabilized austenitic stainless steel was developed as AGR fuel cladding material. The composition of 20Cr25NiNb is shown in Table 1.

### 2.2 Heat treatment

According to the existing literature, the following heat treatment process is generally selected for AGR cladding (Norris, 1987; Powell et al., 1988; Ashworth et al., 1992; Barcellini et al., 2018; Barcellini et al., 2019a; Barcellini et al., 2019b): solution annealing at 1,050°C, then 20%–30% cold processing, and finally annealing at 930°C for 0.5 or 1 h in an inert atmosphere (e.g., hydrogen). The purpose of final annealing is to precipitate NbC in the matrix and “capture” the free C as much as possible to avoid the precipitation of Cr<sub>23</sub>C<sub>6</sub> phase at the grain boundary after aging (Al-Shater et al., 2017). At 930°C, the volume fraction of NbC particles reaches the peak during recrystallization process (Barcellini et al., 2019a).

## 3 Degradation behavior effected by CO<sub>2</sub>

### 3.1 Oxidation

With different exposure temperatures, oxidation regimes can be divided into three categories (Bennett, 1988; Bennett et al., 2014):

1. At temperature  $\leq 925^\circ\text{C}$ , protective Cr<sub>2</sub>O<sub>3</sub> film is formed on the surface of steel, which can maintain good oxidation protection even after long-term isothermal exposure; But the scale exceeding the critical thickness will flake off and fail in the cooling process, then cause pitting.

2. In the range of 950°C–1150°C, internal attack characterized by intergranular silica intrusions happens. Another significant difference is that the Cr<sub>2</sub>O<sub>3</sub> layer would be destroyed by the loss of adhesion of the scale during the isothermal exposure, leading to non-protective attack (LobbEvans, 1987).

3. At higher temperature ranges, oxidation is essentially unprotected.

An amorphous silica with thickness of tens of nanometers between the chrome oxide and the austenitic matrix could be observed for 20Cr25NiNb containing Si (Bennett et al., 1984). The presence of silica makes itself replace Cr<sub>2</sub>O<sub>3</sub> to control the oxidation process, and finally sharply reduces the oxidation rate (Evans et al., 1983). Gray, S (24) et al. found the alloys containing 0% Si and 0.76% Si (wt%) both obey parabolic growth kinetics with the oxidation rate constant of  $3.90 \times 10^{-17} \text{ m}^2 \text{ s}^{-1}$  and  $1.38 \times 10^{-17} \text{ m}^2 \text{ s}^{-1}$ , respectively. The oxide layer that controls the oxidation rate can be transferred (Atkinson, 1986), but in any case the chromium layer thickness increases with time in a parabolic shape (Evans et al., 1978; Emsley and Hill, 1990).

Spallation of oxides during cooling can have serious consequences, not only leading to the occurrence of pitting, but also dispersing the oxides along the entire primary circuit and increasing the loop radioactivity. The strain energy reached a critical value due to the thermal shrinkage difference between the oxide layer and the metal during cooling, which was the cause of spallation (Evans, 1988). The SiO<sub>2</sub> interlayer does not have a great effect on the growth stress of the oxide layer (Gray et al., 2004).

Due to the nail of grain boundaries by carbide precipitated during oxidation, the grain size of oxidized samples did not increase significantly (Bennett et al., 2014). Cyclic heating and cooling of 20Cr25NiNb (1% CO/CO<sub>2</sub>, 900°C–700°C) could show a faster corrosion oxidation process (Osgerby et al., 2001).

### 3.2 Carbon deposition

Impurity gases in the CO<sub>2</sub> medium have significant effects on the oxidation behavior and carbon deposition process. The oxygen potential of CO<sub>2</sub>/1% CO coolant is sufficient to form protective chromium film. But under conditions of high carbon

activity and low oxygen potential (such as containing trace hydrocarbons), 20Cr25NiNb can significantly carburize and deposit carbon, which finally leads to the growth of long filamentous carbon and the release of metal particles (i.e., “metal dusting”) to have harmful effects on heat transfer (Millward et al., 2009).

Nickel has obvious catalytic effect on carbon deposition under environmental oxidation (Millward et al., 2003). A catalytic mechanism was proposed (Millward et al., 2001): in the early stages of exposure, chromium and iron oxidize, but nickel does not, resulting in the residual metals in the surface becoming increasingly Ni-rich, which eventually reaches a stage where pure Ni particles are embedded in the oxide. The establishment of the nickel-catalytic mechanism means carbon deposition could be reduced or avoided by increasing the oxygen potential of the deposited gas (Millward et al., 2009) or adding COS (Taylor et al., 2017) to change the chemical properties of the catalyst.

## 4 Degradation behavior effected by irradiation

After neutron irradiation in the reactor, 20Cr25NiNb will suffer from a series of performance degradation problems, including helium embrittlement, fission gas products and irradiation sensitization. The generation of helium bubbles during thermal neutron irradiation is the most important factor affecting the safety of claddings during service, which leads to the loss of the high temperature ductility, namely “helium embrittlement”. It was early thought to be related to the thermal neutron transmutation reaction of boron. An interesting phenomenon is the alloy with the worst creep performance after irradiation does not have the highest grain boundary boron content probably due to the beneficial effect of untransmuted boron on mechanical properties (Bullough and Jenkins, 1987). Helium bubbles were later found to be more closely related to nickel transmutation (Weitman et al., 1970; Bauer and Kangilaski, 1972; Manley and Rhodes, 1973), and the concentration of helium produced by  $\text{Ni}^{58}(n,\gamma)\text{Ni}^{59}(n,\alpha)\text{Fe}^{56}$  reaction is about 10 times that produced by  $\text{B}^{10}(n,\alpha)$  reaction in 20Cr25NiNb (Bauer and Kangilaski, 1972). A sufficient number of helium bubbles are formed in the grain when irradiated at high temperature (>900 K), while just a small number of voids formed at low temperature (673 K) (Manley and Rhodes, 1973). At high stress, the largest helium bubbles at grain boundaries can be used as a creep cavity nuclei, which are formed at the grain edge (triple point) first and differently produced mainly through coalescence at low stress (Baker et al., 1987).

Another notable change under neutron irradiation is the production of iodine vapor by fission, which could promote

intergranular corrosion on the inner surface of the cladding (Lobb, 1978) and help to “break down” the initially protective  $\text{Cr}_2\text{O}_3$  film, exposing the newly exposed metal to rapid corrosion attack (Lobb, 1981). The breakdown and subsequent regeneration of the  $\text{Cr}_2\text{O}_3$  layer leads to Cr depletion, which promotes the occurrence of radiation-induced segregation (RIS).

Some recent studies focus on RIS or irradiation sensitization. Asymmetric distribution of elements on both sides of grain boundaries was observed under neutron irradiation, which occurred in the temperature range of 350°C–520°C, with peak effects at 420°C (Barcellini et al., 2019b). Chromium depletion at grain boundaries and an increase in intragranular misorientation angles, accompanied by an increase in nanohardness, were observed after 2.2 MeV proton irradiation (Alshater et al., 2018). Local solute redistribution was observed at the defect sink (i.e., grain boundaries, irradiation induced dislocations, and second phase particles) under proton irradiation (Barcellini et al., 2019c): depletion of Cr, Fe, and Mn and segregation of Ni and Si.

## 5 Degraded behavior during long term high temperatures service

The matrix of 20Cr25NiNb annealed at 930°C is usually a single austenite with a few coarse particles (mostly primary NbC particles). In the subsequent high temperature aging, the main precipitates are  $\text{M}_{23}\text{C}_6$ , M(C,N),  $\sigma$  phase and G phase.  $\text{M}_{23}\text{C}_6$  is thermodynamically unstable and the precipitation of G phase in the local region leads to the stoichiometric conditions for the formation of  $\text{M}_{23}\text{C}_6$  (Powell et al., 1988). M(C, N) (M = Nb, V, Ti or Ta) has a fcc structure and a coherent relationship with the austenitic matrix ( $\gamma$ ) (Zhao et al., 2018). The nano-scale M(C,N) precipitated during aging is mainly distributed in the grain and not easy to coarsening, which is considered to be one of the main sources of creep resistance of advanced stainless steels (Sourmail, 2001; Yamamoto et al., 2011). The primary Nb(CN) at grain boundaries is not stable (Ecob et al., 1987) and is usually transformed into a nickel-niobium-silicide phase ( $\text{Nb}_6\text{Ni}_1\text{Si}_7$ , G phase) after aging. The  $\sigma$  phase is a hard and brittle intermetallic compound (Hänninen et al., 1984) consisting mainly of Cr and Fe. After long term aging, the  $\sigma$ -phase network and solute depletion zone gradually formed at grain boundaries degrade the mechanical properties, so the suppression of  $\sigma$  phase is the key to further improve the creep properties (Zhao et al., 2018). The second phase of 20Cr25NiNb is precipitated in the following order during long term aging (Figure 1) (Powell et al., 1988): At grain boundaries,  $\text{M}_{23}\text{C}_6$  precipitates after 200 h, G phase after 500 h, and  $\sigma$  phase after 1000 h. In the matrix, Nb(CN) precipitates after 200 h, followed

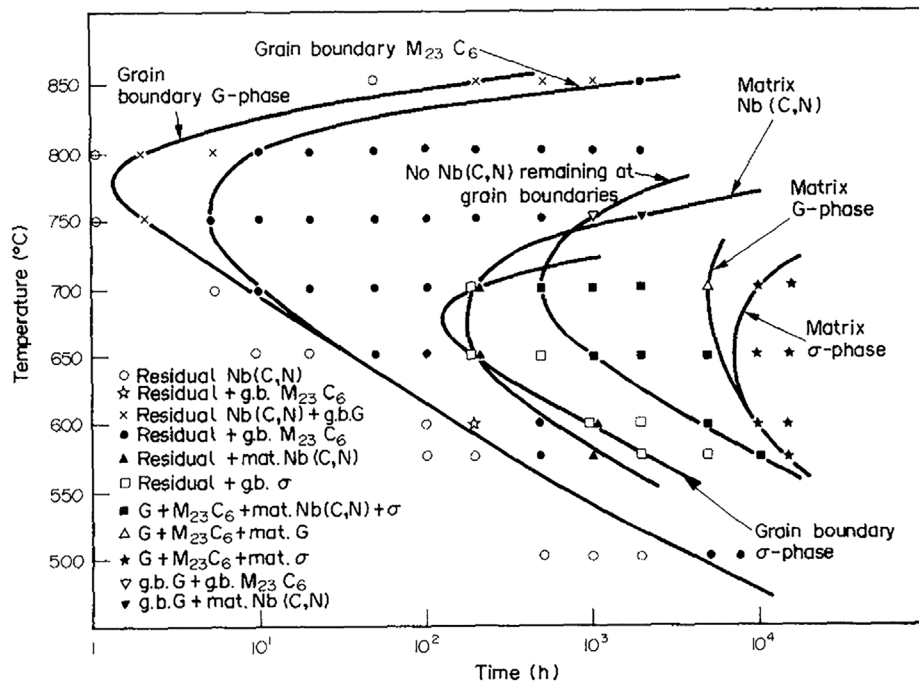


FIGURE 1

TTP (time-temperature-precipitation) diagram of aging process of 20Cr25NiNb at 500°C–850°C (Powell et al., 1988).

by G phase and  $\sigma$  phase. The  $\sigma$  phase precipitates slowly (Jang et al., 2017) and is greatly influenced by the alloy composition (Minami et al., 1986).

The evolution of precipitated phases lead to the degradation of mechanical properties after prolonged aging. The tensile strength of 20Cr25NiNb containing Mo and N elements first rising (0 h–3,000 h) and then decreasing (3,000 h–5,000 h) during aging, with the impact absorption energy sharply dropping (Liang et al., 2016). The steady state creep rate of 20Cr25NiNb at 1123 K can be expressed as  $\dot{\epsilon}_{ss} = A(\sigma - \sigma_0)^p$  (Ecob, 1984).

Jiang. (2018) systematically studied the thermal sensitization behavior of 20Cr25NiNb used for AGR, and found that Si containing alloys exhibited more severe Cr depletion at grain boundaries during sensitization. After annealing at 1,050°C and aging at 650°C for 24 h, the chromium depletion at grain boundaries is similar to that under neutron irradiated.

## 6 Degradation behavior in spent fuel pool

AGR spent fuel will undergo temporary wet storage prior to disposal at the reprocessing plant (Standing, 2001). As

mentioned above, 20Cr25NiNb is sensitized under high temperature and irradiation, so IGSCC and IGA problems exposed to spent fuel pools will be worth considering (Howett et al., 2017). Examples of IGA have been reported in AGR power stations (Norris et al., 1992; Phuah, 2012; Chan et al., 2015; Laferrere et al., 2017). A spent fuel pool containing 1 ppm Cl<sup>-</sup> concentration (pH = 11.4) could not provide protection against corrosion for unsensitized cladding samples at 90°C. Most recent work for degradation behavior in spent fuel pool used electrochemical methods (Al-Shater et al., 2017) (Anwyl et al., 2016) (Phuah, 2012) and multiscale characterization (Clark et al., 2020).

## 7 Conclusion

In this paper, the performance degradation behavior of 20Cr25NiNb cladding material of AGR is reviewed in detail, which has a strong guiding role for the material selection and performance test of sCO<sub>2</sub> cladding.

The degradation behavior mainly includes high-temperature creep, thermal aging, and performance degradation caused by irradiation (including helium embrittlement, fission gas products and irradiation sensitization) and CO<sub>2</sub> (oxidation and carbon deposition). The long-term high temperature service leads to the

evolution of the second phases (especially coarsening of  $\sigma$  brittleness), coupled with irradiation and CO<sub>2</sub> exposure, which makes the mechanical properties degrade faster than those outside the reactor.

An easily overlooked point is IGSCC and IGA of spent fuel during wet storage, on which there has been little research for sCO<sub>2</sub> cladding candidates. (Taylor et al., 2017).

## Author contributions

MS has selected data and written the paper. YS and JX developed the scope of the review and participated in writing the section Introduction. QZ provided guidance and revised manuscript. ZM and XL participated in proofreading and part of the writing.

## Funding

This work was financially supported by the National Key R&D Program of China (grant no. 2020YFB1901800) and the

## References

- Al-Shater, A., Engelberg, D., Lyon, S., Donohoe, C., Walters, S., Whillock, G., and Sherry, A. (2017). Characterization of the stress corrosion cracking behavior of thermally sensitized 20Cr-25Ni stainless steel in a simulated cooling pond environment. *J. Nucl. Sci. Technol.* 54 (7), 742–751. doi:10.1080/00223131.2017.1309305
- Alshater, A. F., Engelberg, D. L., Donohoe, C. J., Lyon, S. B., and Sherry, A. H. (2018). Proton irradiation damage in cold worked Nb-stabilized 20Cr-25Ni stainless steel. *Appl. Surf. Sci.* 454, 130–137. doi:10.1016/j.apsusc.2018.05.128
- Anwyl, C., Boxall, C., Wilbraham, R., Hambley, D., and Padovani, C. (2016). Corrosion of AGR fuel pin steel under conditions relevant to permanent disposal. *Procedia Chem.* 21, 247–254. doi:10.1016/j.proche.2016.10.035
- Ashworth, M. A., Norris, D. I. R., and Jones, I. P. (1992). RADIATION-INDUCED segregation in FE-20CR-25NI-NB based austenitic stainless-steels. *J. Nucl. Mater.* 189 (3), 289–302. doi:10.1016/0022-3115(92)90383-v
- Atkinson, H. V. (1986). Rate controlling factors in the oxidation of 20Cr/25Ni/Nb-stabilized cagr stainless-steel fuel cladding. *Nucl. Energy-Journal Br. Nucl. Energy Soc.* 25 (3), 149–155.
- Baker, C., Beere, W., Callen, V. M., and Clay, B. D. (1987). *The relationship between microscopic helium bubbles and the mechanism of fracture in 20/25/Nb AGR fuel cladding*. London, UK: British Nuclear Energy Society. doi:10.1680/mfncrav1.13063.0001
- Barcellini, C., Dumbill, S., and Jimenez-Melero, E. (2018). Isothermal annealing behaviour of nuclear grade 20Cr-25Ni austenitic stainless steel. *Mater. Charact.* 145, 303–311. doi:10.1016/j.matchar.2018.08.057
- Barcellini, C., Dumbill, S., and Jimenez-Melero, E. (2019). Recrystallisation behaviour of a fully austenitic Nb-stabilised stainless steel. *J. Microsc.* 274 (1), 3–12. doi:10.1111/jmi.12776
- Barcellini, C., Harrison, R. W., Dumbill, S., Donnelly, S. E., and Jimenez-Melero, E. (2019). Evolution of radiation-induced lattice defects in 20/25 Nb-stabilised austenitic stainless steel during *in-situ* proton irradiation. *J. Nucl. Mater.* 514, 90–100. doi:10.1016/j.jnucmat.2018.11.019
- Barcellini, C., Harrison, R. W., Dumbill, S., Donnelly, S. E., and Jimenez-Melero, E. (2019). Local chemical instabilities in 20Cr-25Ni Nb-stabilised austenitic stainless steel induced by proton irradiation. *J. Nucl. Mater.* 518, 95–107. doi:10.1016/j.jnucmat.2019.02.035
- Bauer, A. A., and Kangilaski, M. (1972). Helium generation in stainless steel and nickel. *J. Nucl. Mater.* 42 (1), 91–95. doi:10.1016/0022-3115(72)90011-6

Natural Science Foundation of Sichuan Province (grant no. 2022NSFSC1191).

## Conflict of interest

The authors declare that the research was conducted in the absence of any commercial or financial relationships that could be construed as a potential conflict of interest.

## Publisher's note

All claims expressed in this article are solely those of the authors and do not necessarily represent those of their affiliated organizations, or those of the publisher, the editors and the reviewers. Any product that may be evaluated in this article, or claim that may be made by its manufacturer, is not guaranteed or endorsed by the publisher.

- Bennett, M. J. (1988). Beneficial and detrimental effects of silica in the high temperature oxidation of 20Cr/25Ni/Nb stainless steel. *Key Eng. Mater* 20–28, 3761–3770. doi:10.4028/www.scientific.net/KEM.20-28.3761
- Bennett, M. J., Desport, J. A., and Labun, P. A. (1984). Analytical electron microscopy of a selective oxide scale formed on 20% Cr-25% Ni-Nb stainless steel. *Oxid. Mater.* 22 (5-6), 291–306. doi:10.1007/bf00656580
- Bennett, M. J., Roberts, A. C., Spindler, M. W., and Wells, D. H. (2014). Interaction between oxidation and mechanical properties of 20Cr–25Ni–Nb stabilised stainless steel. *Mater. Sci. Technol.* 6 (1), 56–68. doi:10.1179/mst.1990.6.1.56
- Bullough, C. K., and Jenkins, J. K. (1987). *Helium embrittlement of stabilized 20% Cr 25%Ni stainless steels*. London, UK: British Nuclear Energy Society. doi:10.1680/mfncrav1.13063.0002?src=recsys
- Cao, G., Firouzdar, V., Sridharan, K., Anderson, M., and Allen, T. R. (2012). Corrosion of austenitic alloys in high temperature supercritical carbon dioxide. *Corros. Sci.* 60, 246–255. doi:10.1016/j.corsci.2012.03.029
- Chan, C. M., Engelberg, D. L., and Walters, W. S. (2015). “Performance characterisation of AGR fuel cladding relevant to long-term in-pond storage in pH-moderated aqueous environment,” in Proceedings of the Reactor Fuel Performance - TopFuel 2015, Zurich, Switzerland.
- Clark, R. N., Searle, J., Martin, T. L., Walters, W. S., and Williams, G. (2020). The role of niobium carbides in the localised corrosion initiation of 20Cr-25Ni-Nb advanced gas-cooled reactor fuel cladding. *Corros. Sci.* 165, 108365. doi:10.1016/j.corsci.2019.108365
- Dawson, J. W., and Phillips, M. (2012). Gas-cooled nuclear reactor designs, operation and fuel cycle. *Nucl. Fuel Cycle Sci. Eng.* 300–332. doi:10.1533/9780857096388.3.300
- Dostál, V. (2004). in *Supercritical carbon dioxide cycle for next generation nuclear reactors*. Cambridge, MA USA. Massachusetts Institute of Technology Available at: <https://www.semanticscholar.org/paper/A-supercritical-carbon-dioxide-cycle-for-next-Dost%C3%A1l/7fcb9cd1aa5e086962347d1f74e79202cb558741>.
- Ecob, R. C., Lobb, R. C., and Kohler, V. L. (1987). The formation of G-phase in 20/25 Nb stainless steel AGR fuel cladding alloy and its effect on creep properties. *J. Mat. Sci.* 22 (8), 2867–2880. doi:10.1007/bf01086484
- Ecob, R. C. (1984). Steady state creep of 20% Cr-25% Ni stainless steel with and without a dispersion of tin particles. *Acta Metall.* 32 (12), 2149–2162. doi:10.1016/0001-6160(84)90158-5

- Emsley, A. M., and Hill, M. P. (1990). Intergranular oxidation of silicon in 20Cr-25Ni niobium-stabilized stainless steel at 1140–1230 K. *Oxid. Mater.* 34 (3-4), 351–360. doi:10.1007/bf00665023
- Evans, H. E., and Donaldson, A. T. (1998). Silicon and chromium depletion during the long-term oxidation of thin-sectioned austenitic steel. *Oxid. Metals* 50 (5-6), 457–475. doi:10.1023/a:1018808925756
- Evans, H. E., Hilton, D. A., Holm, R. A., and Webster, S. J. (1983). Influence of silicon additions on the oxidation resistance of a stainless steel. *Oxid. Mater.* 19 (1), 1–18. doi:10.1007/bf00656225
- Evans, H. E., Hilton, D. A., Holm, R. A., and Webster, S. J. (1978). The influence of a titanium nitride dispersion on the oxidation behavior of 20%Cr-25%Ni stainless steel. *Oxid. Mater.* 12 (6), 473–485. doi:10.1007/bf00603805
- Evans, H. E. (1988). Spallation of oxide from stainless steel AGR nuclear fuel cladding: Mechanisms and consequences. *Mater. Sci. Technol.* 4 (5), 414–420. doi:10.1179/mst.1988.4.5.414
- Gray, S., Berriche-Bouhanek, K., and Evans, H. E. (2004). Oxide growth stresses in an austenitic stainless steel determined by creep extension. *Mater. Sci. Forum*, 461–464. 755–764. doi:10.4028/www.scientific.net/MSF.461-464.755
- Hänninen, H., Klemetti, K., and Kivilahti, J. (1984). The effect of sigma phase formation on the corrosion and mechanical properties of Nb-stabilized stainless steel cladding. *Weld. J.* 63 (1), 17–25.
- Haynes, T. A., Podgurschi, V., and Wenman, M. R. (2018). The impact of azimuthally asymmetric carbon deposition upon pellet-clad mechanical interaction in advanced gas reactor fuel. *J. Nucl. Mater.* 513, 62–70. doi:10.1016/j.jnucmat.2018.10.047
- Holcomb, G. R., Camey, C., and Doğan, Ö. N. (2016). Oxidation of alloys for energy applications in supercritical CO<sub>2</sub> and H<sub>2</sub>O. *Corros. Sci.* 109, 22–35. doi:10.1016/j.corsci.2016.03.018
- Howett, E., Boxall, C., and Hambley, D. (2017). AGR cladding corrosion: Investigation of the effect of temperature on unsensitized stainless steel. *Mrs Adv.* 2 (11), 615–620. doi:10.1557/adv.2016.651
- Jang, M.-H., Kang, J.-Y., Jang, J. H., Lee, T.-H., and Lee, C. (2017). Improved creep strength of alumina-forming austenitic heat-resistant steels through W addition. *Mater. Sci. Eng. A* 696, 70–79. doi:10.1016/j.msea.2017.04.062
- Jiang, S. (2018). *Thermally induced sensitisation of austenitic stainless steel for AGR fuel cladding*. Birmingham, UK: University of Birmingham Available at: <https://www.semanticscholar.org/paper/Thermally-induced-sensitisation-of-austenitic-steel-Jiang/190b1dfd688c821df098cbccc1951a72068ccc65>.
- Laferriere, A., Burrows, R., Glover, C., Clark, R. N., Payton, O., Picco, L., and Stacy, M. (2017). *In situ* imaging of corrosion processes in nuclear fuel cladding. *Corros. Eng. Sci. Technol.* 52 (8), 596–604. doi:10.1080/1478422x.2017.1344038
- Liang, Z., Sha, W., Zhao, Q., Wang, C., Wang, J., and Jiang, W. (2016). The effect of aging heat treatment on the microstructure and mechanical properties of 10Cr20Ni25Mo1.5NbN austenitic steel. *High Temp. Mater. Process.* 35 (1), 1–7. doi:10.1515/htmp-2014-0155
- Lobb, R. C. (1981). Observations on the microstructure of 20Cr-25Ni-Nb stainless steel after exposure to iodine vapor during creep at 750°C. *Oxid. Mater.* 15 (1), 147–167. doi:10.1007/bf00603759
- Lobb, R. C. (1978). The effect of iodine vapour on creep rupture properties of nitrided 20% Cr/25% Ni/Nb/1.5 Ti stainless steel. *J. Nucl. Mater.* 74 (2), 212–220. doi:10.1016/0022-3115(78)90360-4
- LobbEvans, R. C. H. E. (1987). The high-temperature oxidation of AGR fuel cladding. *Mater. Nucl. React. core Appl.* 1, 335–340. doi:10.1680/mfncav1.13063.0051
- Manley, A. J., and Rhodes, D. (1973). *12. Helium generation and distribution in thermal reactor irradiated 20 % Cr, 25 % Ni, Nb stabilized stainless steel*. London, UK: British Nuclear Energy Society. doi:10.1680/ieacifacc.48748.0015
- Millward, G. R., Evans, H. E., Aindow, M., and Mowforth, C. W. (2001). The influence of oxide layers on the initiation of carbon deposition on stainless steel. *Oxid. Metals* 56 (3), 231–250. doi:10.1023/a:1010320727492
- Millward, G. R., Evans, H. E., Jones, I. P., and Eley, C. D. (2003). Carbon deposition on stainless steel in oxidising environments. *Mater. A. T. High. Temp.* 20 (4), 535–541. doi:10.1179/mht.2003.062
- Millward, G. R., Evans, H. E., Jones, I. P., Eley, C. D., and Simpson, K. A. (2009). Burn-off of filamentous carbon and subsequent re-deposition on a 20Cr25Ni austenitic steel. *Mater. A. T. High. Temp.* 26 (1), 57–61. doi:10.3184/096034009x436330
- Minami, Y., Kimura, H., and Ihara, Y. (1986). Microstructural changes in austenitic stainless-steels during long-term aging. *Mater. Sci. Technol.* 2 (8), 795–806. doi:10.1179/mst.1986.2.8.795
- Norris, D., Baker, C., Taylor, C., and Titchmarsh, J. (1992). Radiation-induced segregation in 20Cr/25Ni/Nb stainless steel. *ASTM Spec. Tech. Publ.* 189 (3), 603–620. doi:10.1016/0022-3115(92)90383-V
- Norris, D. (1987). “Radiation-induced sensitisation of stainless steels,” in Proceedings of the Symposium on radiation-induced sensitisation of stainless steels, Berkeley, UK.
- Osgerby, S., Evans, H. E., and Saunders, S. (2001). Cracking and spallation of chromia and alumina scales during thermal cycling. *Mater. Sci. Forum*, 369–372. 491–498. doi:10.4028/www.scientific.net/MSF.369-372.491
- Puah, C. H. (2012). “Corrosion of thermally-aged advanced gas-cooled reactor fuel cladding.” Doctor of Philosophy (PhD) (London UK: Imperial College London). doi:10.25560/10550
- Powell, D. J., Pilkington, R., and Miller, D. A. (1988). The precipitation characteristics of 20% Cr/25% Ni/Nb stabilised stainless steel. *Acta Metall.* 36 (3), 713–724. doi:10.1016/0001-6160(88)90105-8
- Sourmail, T. (2001). Precipitation in creep resistant austenitic stainless steels. *Mater. Sci. Technol.* 17, 1–14. doi:10.1179/026708301101508972
- Standing, P. N. (2001). *The long term storage of advanced gas-cooled reactor (AGR) fuel*. Cumbria, UK: British Nuclear Fuels pic, 215–220 Available at: <https://www.osti.gov/etdweb/biblio/681756>.
- Taylor, M., Evans, H., Smith, P., Ding, R., Chiu, Y. L., Rai, S., and Mowforth, C. (2017). The effect of temperature and carbonyl sulphide on carbon deposition on 20Cr25Ni stainless steel. *Oxid. Mater.* 87 (5-6), 667–678. doi:10.1007/s11085-017-9723-7
- Wang, Z., Zhu, Y., Zhu, Y., and Shi, Y. (2016). Energy structure change and carbon emission trends in China. *Energy* 115, 369–377. doi:10.1016/j.energy.2016.08.066
- Weitman, J., Daverhoeg, N., and Farvolden, S. (1970). Anomalous helium production in nickel. *Nucl. Sci. Eng.* 69 (1).
- Whillock, G., Hands, B. J., Majchrowski, T. P., and Hambley, D. I. (2018). Investigation of thermally sensitised stainless steels as analogues for spent AGR fuel cladding to test a corrosion inhibitor for intergranular stress corrosion cracking. *J. Nucl. Mater.* 498, 187–198. doi:10.1016/j.jnucmat.2017.10.017
- Yamamoto, Y., Brady, M. P., Santella, M. L., Bei, H., Maziasz, P. J., and Pint, B. A. (2011). Overview of strategies for high-temperature creep and oxidation resistance of alumina-forming austenitic stainless steels. *Metall. Mat. Trans. A* 42 (4), 922–931. doi:10.1007/s11661-010-0295-2
- Zhao, W. X., Zhou, D. Q., Jiang, S. H., Wang, H., Wu, Y., Liu, X. J., and Lu, Z. P. (2018). Ultrahigh stability and strong precipitation strengthening of nanosized NbC in alumina-forming austenitic stainless steels subjected to long-term high-temperature exposure. *Mater. Sci. Eng. A* 738, 295–307. doi:10.1016/j.msea.2018.09.081